Available online at www.sciencedirect.com

ScienceDirect

Procedia CIRP 74 (2018) 628–631

www.elsevier.com/locate/procedia

10th CIRP Conference on Photonic Technologies [LANE 2018]

Time-resolved detection of vaporization during laser metal processing with laser-induced fluorescence

Brian J. Simonds[a,*], Paul Williams[a], John Lehman[a]

[a]*National Institute of Standards and Technology, 325 Broadway, Boulder, CO 80305 USA*

* Corresponding author. Tel.: +1-303-497-3270. *E-mail address:* brian.simonds@nist.gov

Abstract

Element loss during high-power laser processing of metals can lead to deleterious chemical and mechanical effects that negatively impact the processed material's quality. Currently, there is no suitable way to measure time-resolved element loss *in situ* during laser processing. In this work, we show that laser-induced fluorescence (LIF) can be used to temporally resolve individual element vaporization during a laser spot welding of 316L stainless steel. As a proof-of-concept, we measured iron loss during a 500 µs laser spot weld with a time resolution of 5 microseconds. We found that keyhole formation could clearly be identified by a dramatic increase in iron emission from the weld pool. This conclusion was validated by independent, time-resolved measurements of laser absorptance during laser spot welding from our previous work.

Keywords: Laser welding; Applied spectroscopy; Laser-induced slourescence

1. Introduction

Laser processing of metals can lead to disproportional alloy element loss due to the differences in vapor pressures among the constituent elements. For instance, several researchers have found evidence where the relative loss of a single element has led to mechanical and microstructural changes during laser welding [1–9]. However, these works all relied on destructive, *ex situ* analysis to make this determination. A more useful technique for monitoring vapor element loss is one that is both *in situ* and real-time such that feedback process control is possible. These requirements suggest that a non-contact optical technique should be used.

Previous efforts of optically resolving element loss have relied on optical emission spectroscopy (OES) whereby laser weld plume light is spectroscopically resolved [10–15]. The sensitivity of OES limits its ability to identify any but the most abundant elements coming from the weld pool. Increasing the signal-to-noise of OES is possible with increased integration, but this would degrade temporal resolution precluding its use as a real-time monitoring system.

In a previous work, we demonstrated that laser-induced fluorescence (LIF) can be used during the laser weld process and is 40,000 times more sensitive than OES alone allowing for low concentration alloy element loss detection [16]. In this work, we show that by gating the 5 ns LIF excitation laser pulse a time-resolved, element specific signal can be generated. This is the first step toward developing a real-time, element specific vaporization monitoring technique. Iron is used for this demonstration as it gives the strongest signal due to its relative abundance and is common in many welded materials.

10.1016/j.procir.2018.08.072

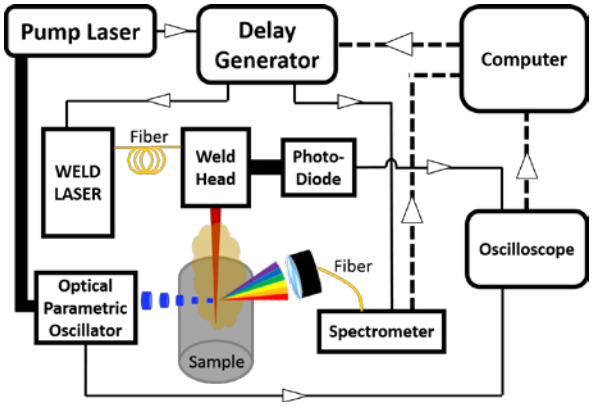

Fig. 1. A flow diagram of the experimental configuration. The thin, solid lines represent timing signals; the dashed lines are data or command signals; and the thick black lines are concealed beam tubes.

2. Experimental Arrangement

Weld plume emissions were measured during 0.5 ms laser spot welding of 316L stainless steel. This sample was in pipe form with 10.2 mm outer diameter and 6.35 mm thick walls. The laser welds were performed with a fiber laser operating at 1070 nm with output powers from 1020 W to 2240 W (0.51 J to 1.12 J in 0.5 ms). All spot welds were made with the sample at the focal plane of the weld laser where the beam profile was radially symmetric and top-hat with a full-width at half maximum diameter of 510 µm.

The basic experimental apparatus for LIF was detailed in a previous publication [16]. Briefly, fluorescence was induced by a pulsed laser incident to the weld plume, which was wavelength-tuned to a resonant absorption transition in the element of interest. This pulse was produced by an optical parametric oscillator (OPO) that was pumped by a wavelength

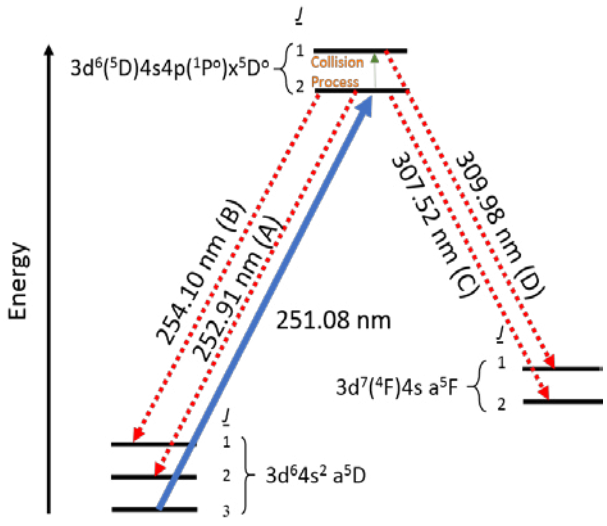

Fig. 2. An atomic energy diagram for the iron transitions used in this study. The pump transition is at 251.08 nm (solid, blue line) with the optical emissions seen given with the dashed red lines. The letters in parenthesis correspond to the spectral peaks in Fig. 3.

tripled Nd:YAG laser operating at a 10 Hz repetition rate.

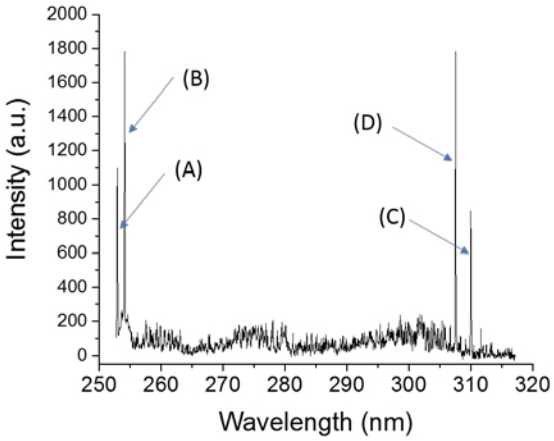

Fig. 3. A typical laser-induced fluorescence spectrum taken with a delay time of 144.6 µs. The four marked peaks are from iron pumped at 251.08 nm. The letters correspond to the transitions shown in Fig. 2.

The fluorescence signal from the targeted species was then collected and sent to a high-resolution spectrometer where it was wavelength resolved.

The time-resolved LIF measurements were obtained by controlling the delay time between the laser weld pulse and OPO pump laser pulse. This was achieved by using a delay generator whose internal time reference was linked to the OPO pump laser. The delay generator triggered both the weld laser and the spectrometer shutter. A computer controlled the time delay between when the OPO fires a pulse and when the weld laser fires. The actual weld laser emission was measured with a photodiode mounted to the laser weld head. This signal was sent to a fast oscilloscope along with a signal from the OPO pulse so that the actual delay time could be measured for each LIF signal. This value and the collected spectra were sent to a computer to be analyzed. The time resolution of this experimental arrangement was 2.5 µs, which was limited by the variation in response of the weld laser to its trigger pulse. At each delay time, 30 individual spectra were captured. The pipe sample was rotated beneath the weld head at 150 °/min. so that a fresh spot was welded for each spectral measurement.

The Fe atomic absorption targeted by the OPO pump laser was at 251.083 nm, which represented a resonant absorption from the $3d^64s^2\ a^5D\ 3$ state to the $3d^6(^5D)4s4p(^1P^o)\ x^5D^o\ 2$ state. This is shown in the atomic energy diagram in Fig. 2 along with the optical relaxation paths seen in our spectra. The letters in parenthesis correspond to the resonant peaks labeled in the spectrum in Fig. 3, which is the average spectrum taken at delay time 144.6 µs. The four most intense peaks were the resonant transitions given in Fig. 2. The background emission (as in, when the OPO was not firing) has been subtracted from this spectrum. The fluorescent signal used for this study was from this excited state to the $3d^64s^2\ a^5D\ 1$ state with a measured spectral peak at 254.10 nm (peak (B)). The 254.10 nm peak of each spectrum was integrated and averaged with 30 similar measurements with the error bars in Fig. 4 representing the standard deviation of these integrated values.

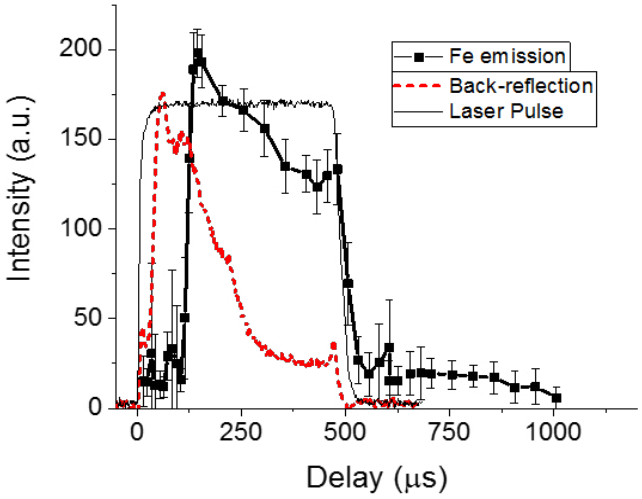

Fig. 4. The integrated intensity of an iron spectral peak plotted as a function of pump delay time (black squares). The solid black line represents the actual weld laser emission. The dashed red line is the weld laser back reflection.

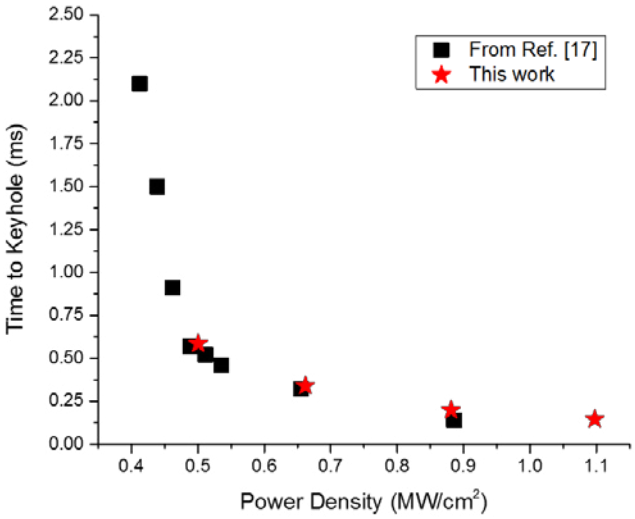

Fig. 6. The time needed for keyhole formation determined by dynamic absorptance measurements during laser spot welding in ref. [17] are given with the black squares. The red stars show those values from this work.

3. Results and Discussion

Figure 4 shows the average integrated intensity of the resonant Fe peak plotted as a function of delay time (black squares) for a 500 µs laser spot weld with 1.12 J (2240 W). Also shown is the actual laser emission (black line) measured by the weld laser photodiode monitor. This shows a temporally stable laser emission with an approximate 50 µs risetime. The dashed red line is the back-reflection to the weld head photodiode during a laser spot weld.

These data reveal several key features of the Fe emission during the laser spot weld. The first is the steep initial rise in intensity starting near 125 µs and peaking at 144.6 µs. This rise coincides with a decrease in the back-reflection monitor signal. This behavior is consistent with a keyhole opening process, as the keyhole results from the intense vaporization that creates a cavity in the molten metal surface due to a recoil force. The creation of the keyhole was accompanied by an increase in absorptance of the weld laser light [17], which was also the cause of the decreasing back-reflected signal.

Once the Fe emission peaks, it steadily declined until the end of the laser pulse. This is interpreted to result from some iron vapor redepositing inside the keyhole as it continues to deepen with prolonged laser exposure thereby lowering the overall amount in the vapor plume. A spectral signal from Fe was clearly visible for times significantly longer than the duration of the weld pulse (between 500 µs and 1000 µs). In fact, the signal-to-noise improved slightly during this time as the weld plume is no longer contributing to background noise. This signal is evidence of evaporation from the molten metal weld pool and should relate to the solidification rate.

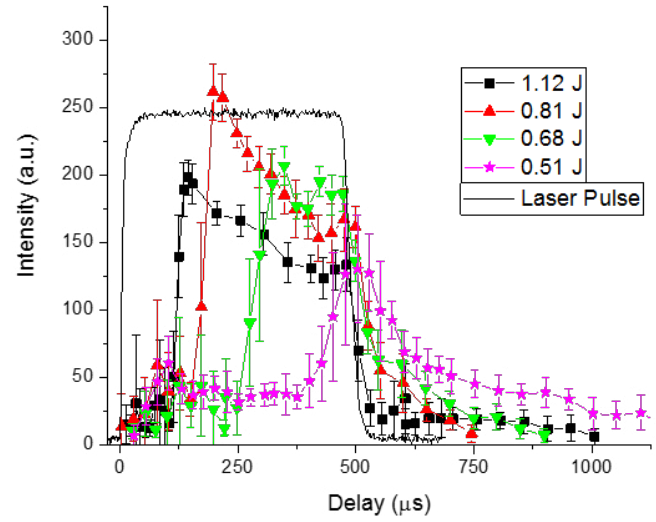

Fig. 5. The time-dependent emission of Fe from the weld pool determined from LIF spectroscopy at different values of weld laser energy. The solid black line represents the temporal profile of the weld laser pulse used for the spot weld.

Figure 5 shows the results from progressively lower weld laser input energy. One first notices that the keyhole formation, as evidenced by the peak in Fe emission, occurred at later times with respect to weld laser illumination as the weld laser energy decreases. A previous publication observed keyhole formation by measuring the time-dependent laser absorptance during a laser spot weld [17]. In that work, the keyhole formation time ("Time-to-Keyhole") was determined by a dramatic increase in absorptance. These results are plotted in Fig. 6 as a function of weld laser power density along with the values determined form this work from the peak intensity of the Fe emission. The excellent agreement of these values over a range of power densities supports our interpretation of the main time-dependent spectral feature as being from keyhole formation.

Additionally, the relative rate at which the keyhole is formed can be observed from Fig. 5. The slope of the intensity leading to the peak emission gradually decreases with decreasing weld laser energy meaning that keyhole formation is not as rapid even once initiated. Also noteworthy is the behavior of the Fe emission once the weld laser pulse has ended. The intensity of the post-weld laser Fe emission increased with lower weld laser energy. We are as yet unable to definitively state the reason for this.

4. Conclusions

We demonstrated that LIF can be used to observe the time-dependence of individual element loss during a 500 µs laser spot weld of 316L stainless steel by monitoring iron emission. The data reveal dynamics of laser welding including keyhole formation and weld pool cooling. These results quantitatively agree with previous work that observes keyhole formation through dynamic absorptance measurements. The ability to spectroscopically measure weld pool dynamics allows for the possibility that such a technique can be used as a real-time, element specific weld pool monitor.

References

[1] Moon DW, Metzbower EA. Laser beam welding on aluminum alloy 5456, Weld. J. 1983;62;53s-58s.
[2] Khan PAA, Debroy T. Alloying element vaporization and weld pool temperature during laser welding of AISI 202 stainless steel. Metall. Trans. B. 1984;15;641-44.
[3] Collur MM, Paul A, Debroy T. Mechanism of alloying element vaporization during laser welding. Metall. Trans. B. 1987;18;733-40.
[4] Khan, PAA, DebRoy T, David SA, Laser Beam Weldign of High-Manganese Stainless Steels – Examination of Alloying Element Loss and Microstructural Changes. Weld. J. – Suppl. 1988;1s-7s.
[5] Mundra K, DebRoy T. Calculation of weld metal composition change in high-power conduction mode carbon dioxide laser-welded stainless steels. Metall. Trans. B. 1993;24;145-55.
[6] Zhao H, DebRoy T. Weld metal composition change during conduction mode laser welding of aluminum alloy 5182. Metall. Mater. Trans. B. 2001;32B;163-72.
[7] Jandaghi M, Parvin P, Torkamany MJ, Sabbaghzadeh J. Alloying element losses in pulsed Nd:YAG laser welding of stainless steel 316. J. Phys. D. Appl. Phys. 2008;41;235503.
[8] He X, Debroy T, Fuerschbach PW. Composition change of stainless steel during microjoining with short laser pulse. J. Appl. Phys. 2004;96;4547-55.
[9] Cieslak MJ, Fuerschbach PW. On the weldability, composition, and hardness of pulsed and continuous Nd:YAG laser welds in aluminum alloys 6061, 5456, and 5086. Metall. Trans. B 1988;19;319-29.
[10] Collur MM, DebRoy T. Emission spectroscopy of plasma during laser welding of AISI 201 stainless steel. Metall. Trans. B. 1989;20B;277-86.
[11] Dasgupta AK, Mazumder J. Laser welding of zinc coated steel: an alternative to resistance spot welding. Sci Technol. Weld. Join. 2008;13;289-93.
[12] Hoffman J, Szymaski Z. Time-depenent spectroscopy of plasma plume under laser welding conditions. J. Phys. D. Appl. Phys. 2004;37;1792-99.
[13] Kong F, Ma J, Carlson B, Kovacevic R. Real-time monitoring of laser welding galvanized high strength steel in lap joint configuration. Opt. Laser Technol. 2012;44;2186-96.
[14] Sibillano T, Ancona A, Berardi V, Lugara PM. Correlation analysis in laser welding plasma. Opt. Commun. 2005;251:139-48.
[15] Szymanski, Hoffman J, Kurzyna J. Plasma plume oscillations during welding of thin metal sheets with a CW CO2 laser. J. Phys. D. Appl. Phys. 2001;34;189-99.
[16] Simonds BJ, Sowards JW, Williams PA. Laser-induced fluorescence applied to laser welding of austenitic stainless steel for dilute alloying element detection. J. Phys. D. Appl. Phys. 2017;50;325602.
[17] Simonds BJ, Sowards JW, Hadler JA, Pfeif EA, Wilthan B, Tanner J, Harris C, Williams PA, Lehman JH. Time-resolved Absorptance and Melt Pool Dynamics during Intense Laser Irradiation of Metal. In Review.